

1 **Typical meteorological conditions associated with extreme nitrogen dioxide**
2 **(NO₂) pollution events over Scandinavia**

3
4 Manu Anna Thomas and Abhay Devasthale

5
6 Research and development department, Swedish Meteorological and Hydrological Institute
7 (SMHI), Folkborgsvägen 17, 60176 Norrköping, Sweden

8 Correspondence: manu.thomas@smhi.se
9

10
11
12 **Abstract**
13

14 Characterizing typical meteorological conditions associated with extreme pollution events helps in
15 the better understanding of the role of local meteorology in governing the transport and distribution
16 of pollutants in the atmosphere. The knowledge of their co-variability could further help to evaluate
17 and constrain chemistry transport models (CTMs). Hence, in this study, we investigate the statistical
18 linkages between extreme nitrogen dioxide (NO₂) pollution events and meteorology over
19 Scandinavia using observational and reanalysis data. It is observed that the south-westerly winds
20 dominated during extreme events, accounting for 50-65% of the total events depending on the
21 season, while the second largest annual occurrence was from south-easterly winds, accounting for
22 17% of total events. The specific humidity anomalies showed an influx of warmer and moisture-
23 laden air masses over Scandinavia in the free troposphere. Two distinct modes in the persistency of
24 circulation patterns are observed. The first mode lasts for 1-2 days, dominated by south-easterly
25 winds that prevailed during 78% of total extreme events in that mode, while the second mode lasted
26 for 3-5 days, dominated by south-westerly winds that prevailed during 86% of the events. The
27 combined analysis of circulation patterns, their persistency, and associated changes in humidity and
28 clouds suggests that NO₂ extreme events over Scandinavia occur mainly due to the long-range
29 transport from the southern latitudes.
30
31
32
33
34

35

36 **1. Introduction**

37

38 Nitrogen dioxide (NO₂) is one of the highly reactive gases of the nitrogen oxides (NO_x) family. The
39 major sources of NO₂ are fuel combustion in motor vehicles, industrial boilers, emissions from soil
40 and agricultural biomass burning. The natural source of NO₂ is lightning and forest fires. Recent
41 studies indicate increasing trends in NO₂ in developing countries and decreasing trends in developed
42 countries as a result of environmental regulation policies (Richter et al. 2005; Zhang et al. 2007; van
43 der A et al. 2008; Schneider et al. 2015; Geddes et al. 2016). NO₂ is an oxidizing agent resulting in
44 the corrosive nitric acid and plays an important role aiding the formation of ozone. It can also
45 contribute to the formation of particulate matter (PM) and secondary organic particles through
46 photochemical reactions. Increased NO_x concentrations not only severely affect human physical
47 health through reduced lung function, but also affect aquatic ecosystems through acid deposition
48 and eutrophication of soil and water (Sjöberg et al. 2004; Klingberg et al. 2009; Bellandar et al.
49 2012; Gustafsson et al. 2014; Nilsson Sommar et al. 2014; Oudin et al. 2016; Taj et al. 2016).
50 According to the fifth IPCC assessment report, the total global NO_x emissions have increased by
51 20% since pre-industrial periods to 324 ppb in 2011. (Lamarque et al., 2013, based on the model-
52 intercomparison project, ACCMIP, assessed increases in regional nitrogen deposition by up to 30-
53 50% from RCP 2.6 to RCP 8.5). In heavily polluted areas NO₂ can also have noticeable impact on
54 the local radiation budget (Vasilkov et al. 2009).

55

56 Compared to other pollutants such as carbon monoxide (CO) that has a life span of weeks to few
57 months, NO₂ has a relatively shorter life time in the atmosphere and ranges typically from a couple
58 of hours in the boundary layer to up to few days in the upper troposphere (Beirle et al., 2011).
59 Therefore, NO₂ can be typically associated with short-range transport events. For long range
60 transport (LRT) or intercontinental transport of pollutants and in particular of NO₂ to occur, the
61 associated weather systems need to be linked with stronger winds and rapid convective-advective
62 events such as cyclones or warm conveyor belts (WCBs) that can lift air masses from their source
63 regions up into the free troposphere and be transported across the oceans (Eckhardt et al. 2003;
64 Stohl et al. 2003). Due to lower concentrations of radical species in the free troposphere, the
65 reaction with NO₂ is limited. Zien et al. (2014) identified about 3800 LRT events of NO₂ during a 5
66 year period from the major pollution hotspots such as the east coast of North America, central
67 Europe, China and South America, predominantly during autumn and winter months.

68

69 There have been several studies reporting individual LRT events of NO₂. To mention a few, Stohl et

70 al. (2003) in a study explained “intercontinental express highways” being responsible for almost
71 60% of the total intercontinental transport of pollutants from across the Atlantic to Europe, resulting
72 in an increment of average European winter NO_x mixing ratios by about 2-3 pptv. In yet another
73 study, Schaub et al. (2005) demonstrated that at least 50 % of the NO₂ recorded at the Alpine region
74 was advected via a frontal system from the Ruhr area in central Germany in February 2001.
75 Donnelly et al. (2015) reported that easterly air masses during winter resulted in increased NO₂
76 concentrations in the urban and rural sites in Ireland. LRT of NO_x across the Indian Ocean from
77 South Africa to Australia in May 1998 was reported by Wenig et al. (2003).

78
79 The Nordic countries often lie at the receiving end of short-range pollutant transport from northern
80 Europe or they are a part of a much larger transit pathway of eventual long-range transport to the
81 Arctic, originating from either Europe or North America. To what extent such a transport from the
82 southerly latitudes affects the characteristics of extreme pollution events (such as magnitude,
83 frequency and persistence) over Scandinavia depends largely on prevailing circulation patterns and
84 meteorological conditions. The local meteorology can enhance or dampen the concentration of the
85 pollutants depending on the degree of persistency; the knowledge of which would help to better
86 constrain the chemistry transport models (CTMs). Therefore, identifying the dominant weather
87 patterns over Scandinavia especially during extreme pollution is important. However, there has not
88 been a systematic study linking the transport events of NO₂ to different meteorological conditions,
89 solely from observational data over the Scandinavian region. Therefore, the main aim of the present
90 study is to characterize circulation regimes and meteorological conditions extreme pollution events,
91 to understand to what extent they differ from climatological conditions. There are two different
92 ways to study this co-variability solely using observational data: 1) the “top- down approach”
93 wherein the atmospheric state is first identified and then the variability of the tracers is evaluated.
94 This approach gives a general perspective of the distribution of tracers based on a particular weather
95 state and 2) the “bottom-up approach” wherein the pollution episode is first identified and the
96 weather state associated with it is studied. In this study we make use of the bottom-up approach as
97 explained in the next section.

98

99

100 **2. Data sets and methodology**

101

102 The NO₂ tropospheric column densities from OMI (Ozone Monitoring Instrument) on board the
103 EOS Aura satellite are used in this study to define and identify extreme events (Boersma et al.,
104 2001, 2008, 2011; Bucsela et al., 2006, 2008, 2013; Lamsal et al. 2008, 2010, 2014). 11 years (2004

105 – 2015) of daily Level 3 gridded standard product, available at 0.25x0.25 degrees resolution is
106 analysed (OMNO2d, Version 3, available at: [https://disc.gsfc.nasa.gov/Aura/data-
108 holdings/OMI/omno2d_v003.shtml](https://disc.gsfc.nasa.gov/Aura/data-
107 holdings/OMI/omno2d_v003.shtml)). This particular product is used as it provides good quality
109 OMI retrievals, already screened based on recommendations by the OMI Algorithm Team. We
110 allowed retrievals under partially cloudy conditions to be analysed, not only to have robust number
111 of samples, but also to avoid clear-sky biases since the NO₂ transport is often associated with
112 cyclonic systems that lead to increased cloudiness (Zien et al. 2014). We further tested the
113 sensitivity of our results to using only cloud screened retrievals, to evaluate if the selection of
114 extreme events and associated meteorological conditions are different from those cases when
115 retrievals under partially cloudy conditions are used.

116 Humidity and cloud fraction retrievals from the AIRS (Atmospheric Infrared sounder) instrument
117 on board Aqua satellite are used (Chahine et al. 2006; Susskind et al. 2014; Devasthale et al. 2016).
118 Both Aqua and Aura satellites are a part of NASA's A-Train convoy, providing added advantage of
119 simultaneous observations of trace gases from OMI-Aura and thermodynamical information from
120 AIRS-Aqua. AIRS Version 6 Standard Level 3 Daily Product (AIRX3STD) for the same period
121 (2004-2015) is used (data available at:
122 <https://disc.gsfc.nasa.gov/uui/datasets?keywords=%22AIRS%22>).

123
124 To investigate circulation patterns, u and v wind components at 850 hPa from ECMWF's ERA-
125 Interim Reanalysis are used (Dee et al., 2011; [http://apps.ecmwf.int/datasets/data/interim-full-
127 daily/levtype=sfc/](http://apps.ecmwf.int/datasets/data/interim-full-
126 daily/levtype=sfc/)).

128 In order to investigate co-variability of meteorological conditions and pollutants using observations,
129 two different approaches can be taken (Fig. 1). In a "top-down" approach, a weather state
130 classification can be done to identify most prevailing weather states that occur over the study area
131 and then the relative distribution of pollutants can be investigated under those states to rank them.
132 This approach was adapted by Thomas and Devasthale (2014) and Devasthale and Thomas (2012).
133 In a "bottom-up" approach on the other hand, a set of pollution events can be identified first and
134 then the corresponding meteorological conditions can be investigated. This bottom-up approach is
135 the focus of the present study. It should be mentioned that both of these approaches have their
136 advantages and limitations. For example, the dominant weather pattern identified in the top-down
137 approach may not have the largest impact on pollutant variability and the pollution events identified
138 in the bottom-up approach may not be associated with the dominant weather pattern or may not
139 have the largest impact on an average in the weather state they occur. Therefore, only the

140 combination of these two approaches will provide a complete picture of the co-variability between
141 meteorological conditions and pollutants.

142

143 In the present study, an “extreme” pollution event is defined as follows. First, the histograms of
144 NO₂ tropospheric column densities using OMI data for each month are computed over the centre of
145 the study area (55N-60N, 11E-20E). This area is chosen because it accommodates top ten polluted
146 and populated cities/regions in Sweden (Sjöberg et al. 2004; Klingberg et al. 2009; Bellandar et al.
147 2012; Gustafsson et al. 2014; Nilsson Sommar et al. 2014; Oudin et al. 2016; Taj et al. 2016). All
148 events that surpass the 90-percentile (90%ile) value are considered as extreme events. The monthly
149 histograms of NO₂ over the study region are shown in Fig. 2 along with 90 percentile thresholds for
150 each month (vertical lines). Since NO₂ distributions over the study area show strong monthly
151 variability, the monthly thresholds were chosen to define extreme events. The distributions of NO₂
152 have longer tails during winter half year and the concentrations are also higher. Therefore, the
153 resulting 90%ile thresholds are also higher in winter compared to summer months. However, using
154 thresholds based on percentiles (rather than having a fixed value throughout the season or year),
155 makes the criteria for the selection of extreme events fair and equally applicable for each month.

156

157 **3. Meteorological conditions observed during extreme events**

158

159 The spatial distribution of tropospheric NO₂ column during climatological conditions, extreme
160 events and anomalies thereof is presented in Fig. 3. Note that although the thresholds for defining
161 extreme events are different for each month, the results are compiled over four distinct seasons for
162 the sake of brevity. By definition, NO₂ anomalies during extreme events are similar in magnitude to
163 climatological values over Scandinavia. The spatial extent of the severity of the extreme pollutant
164 episodes over southern Sweden is noticeable. Under climatological conditions, highest
165 concentrations are observed over northern Germany and France, the Netherlands and Belgium (the
166 Benelux region). There is a good spatial coherence between NO₂ distributions under climatological
167 conditions and extreme events, in the sense that the high concentrations of NO₂ seemed to have
168 spread over southern Scandinavia during extreme events from the regions where climatological
169 values are usually higher. It is to be noted that during extreme events the pollution levels over
170 northern European regions are also enhanced. For an event to qualify as an extreme event over
171 southern Scandinavia, the pollutant levels in the source regions also need to be higher than usual in
172 order to allow strong transport under favourable atmospheric circulation patterns. This provides
173 confidence in the selection process of extreme events. The NO₂ concentrations are relatively higher
174 in winter and autumn compared to the summer months. This is mainly because atmospheric

175 removal by radical species and deposition are much more efficient in the summer months.

176

177 In order to characterize typical meteorological conditions that can result in such high concentrations
178 over Scandinavia, we first investigated the dominant wind direction at 850 hPa associated with
179 those extreme events using ERA-Interim reanalysis data. The normalized frequency of occurrence
180 of different wind directions during four seasons is shown in Fig. 4. It can be seen that, irrespective
181 of the season, the south-westerly winds are dominant during extreme events accounting for 50-65%
182 of total events. This is consistent with south-westerly extension of pollution plume mentioned
183 earlier. The second largest annual occurrence is from south-easterly winds, accounting for 17% of
184 total events followed equally similar contribution from north-westerly winds. Compared to
185 climatological conditions, south-westerly winds have 30-40% more likelihood of being dominant
186 during extreme events depending on the season. However, such clear tendency compared to
187 climatological conditions is not observed in the case of other wind directions. The spatial pattern of
188 the 850 hPa winds based on ERA-Interim reanalysis and corresponding humidity anomalies at 850
189 hPa based on AIRS data during extreme events are shown in Figs. 5 and 6 respectively. A clear
190 transport pathway from the northern continental Europe to Scandinavia is visible. The strongest
191 winds are observed during the DJF months followed by the SON months with average wind speeds
192 reaching over 10 m/s. The weakest winds are observed during the JJA months. The circulation
193 pattern is characterized by the presence of low pressure systems in the Norwegian Sea that create
194 favourable conditions for the transport of pollutants from continental Europe into Scandinavia. The
195 location of the center of these cyclonic systems can slightly vary over the Norwegian Sea, affecting
196 the direction and strength of the northward flow, as evident in Fig. 5. For example, in the DJF
197 months, the center is located far away in the open Norwegian Sea allowing stronger south-westerly
198 winds over southern Scandinavia. In the JJA months, the center of cyclonic systems is close to
199 western Norwegian coast. While this pattern also leads to south-westerly winds, air masses are
200 mixed with colder and drier air from the northern Norwegian Sea.

201

202 The specific humidity anomalies show an influx of warmer and moister air masses over Scandinavia
203 (Fig. 6), except in summer as mentioned above. The seasonality in the vertical structure of the
204 specific humidity anomalies over Scandinavia is shown in Fig. 7c. While there are large deviations
205 in humidity anomalies, influenced by the strength of the wind flow, they are positive regardless of
206 the season during extreme events and peak at 2-3 km above the surface. Such increase in the free
207 tropospheric moisture, especially during winter half year in the absence of local moisture sources,
208 can only be explained by the transport from southern latitudes. The vertical water vapour anomalies
209 are higher in winter half year (DJF and SON), consistent with high NO₂ anomalies during those

210 months. Fig. 8 further shows cloud fraction anomalies. Average cloudiness is increased in all
211 seasons during extreme events, in particular during winter half year. During this time of year, the
212 large-scale frontal systems originating from the southwesterly regions can bring moister airmasses
213 over Scandinavia, as can be seen in the circulation patterns and humidity anomalies, creating
214 favourable conditions for cloud formation. Therefore, these positive cloud fraction anomalies, in
215 combination with positive humidity anomalies and circulation patterns, are indicative of the long-
216 range transport of airmasses associated with increased NO₂ concentrations.

217

218 For an extreme pollution event to be linked with the transport the wind flow should be stronger
219 allowing rapid advection and associated circulation pattern also needs to be persistent. Fig. 7a and
220 7b show the histograms of wind speed at 850 hPa over the study areas during extreme events when
221 data are partitioned by wind direction and by season respectively. The average values of wind
222 speeds are also shown for extreme events and climatological conditions (in brackets). Although the
223 distributions are shifted to higher wind speeds in nearly all cases during extreme events compared
224 to climatological conditions, the average wind speeds are not significantly different. The south-
225 westerly winds are strongest and show largest difference in average wind speeds, while the
226 northeasterly winds are weakest. Average wind speeds during the winter half year (DJF and SON)
227 are higher than the summer half year, consistent with observed positive anomalies of humidity and
228 clouds.

229

230 The persistency of the different circulation patterns during these extreme events is further evaluated
231 as shown in Fig. 7d. The persistency is defined as follows. If an extreme event is observed, the wind
232 speed and wind direction are computed for the last 10 days. It is then checked how many days back
233 in time that particular wind direction was *continuously* sustained. Two distinct modes in the
234 persistency of circulation patterns are observed, one in which a particular wind direction persists for
235 a day or two and a second mode in which winds persists for 3 to 5 continuous days. This is clearly
236 different from the degree of persistency observed under climatological conditions when winds
237 persisted in one particular direction predominantly for few days. It was identified that during
238 extreme events south-easterly winds dominated the first mode explaining 78% of the total
239 occurrence in that mode and the westerly winds dominated the second mode explaining 86% of the
240 total occurrence. In the latter case, when the winds persist for few days (3-5 days), the conditions
241 are favourable for the long-range transport from the southern latitudes since circulation patterns
242 (Fig. 5) are associated with typical frontal systems and baroclinic disturbances that make their way
243 over Scandinavia.

244

245

246 **4. Sensitivity of chosen events to cloud clearing procedure**

247

248 As mentioned in Section 2, we allowed retrievals under partially cloudy conditions to be analysed,
249 not only to have a robust number of samples, but also to avoid potential clear-sky biases. However,
250 clouds can contaminate the NO₂ retrievals by modulating scattering in the atmosphere. Moreover,
251 clouds are highly variable not only in space and time but also in their nature, thus making it
252 challenging to assess their overall impact on the quality of retrievals. In the case of our study,
253 potential cloud contamination can affect the selection of extreme events and thereby associated
254 weather patterns that are being studied. Therefore, we carried out a sensitivity study wherein the
255 entire analysis was repeated using only cloud screened NO₂ retrievals to investigate to what extent
256 cloud clearing would affect the chosen events and subsequent analysis. Fig. 9 shows the histograms
257 of NO₂ total columns under partially cloudy (solid lines) and cloud screened conditions (dotted
258 lines). The histograms are accumulated over four seasons instead of months for clarity (to avoid too
259 many lines). The chosen 90%ile thresholds are certainly different under partially cloudy and cloud
260 screened conditions, but only slightly. We also found that, depending on the month, the selected
261 extreme events match under partially cloudy and cloud screened conditions between 76% and 88%
262 of the time. Fig. 10 further shows the spatial climatological distribution of NO₂ and during extreme
263 events using only cloud screened retrievals. When compared to Fig. 3, the spatial distributions look
264 patchy as a result of selected screening, but the magnitude and spatial features do not change
265 significantly, providing confidence in our earlier analysis based on partially cloudy retrievals.
266 Finally we evaluated if the events based on cloud screened data impact the analysis of
267 meteorological conditions investigated here. Fig. 11 shows the vertical structure of specific
268 humidity anomalies over the study region under partially cloudy (solid lines) and cloud screened
269 conditions (dotted lines). While the slight differences in the vertical structure do exist, their sign and
270 magnitudes are not large enough to change any previous argumentation.

271

272 **5. Conclusions**

273

274 The main aim of the present study was to characterize typical meteorological conditions associated
275 with extreme NO₂ pollution events over Scandinavia. To that end, the study employs the bottom-up
276 approach, in contrast to top-down approach taken by Thomas and Devasthale (2014) to study
277 statistical co-variability of weather states and pollutant distribution. Such detailed analysis
278 characterizing circulation patterns and meteorological conditions involving more than 300 extreme
279 pollution events identified using satellite data has not been done before over the Scandinavian

280 region. It is observed that the south-westerly winds dominated during extreme events accounting for
281 50-65% of total events, while the second largest annual occurrence was from south-easterly winds,
282 accounting for 17% of total events followed by an equally similar contribution from north-westerly
283 winds. Wind speeds are generally higher during extreme events, but only slightly, making it
284 challenging to delineate distinct circulation regimes under these events. For the first time, we
285 investigated the degree of persistency of wind direction during extreme events. In contrast to
286 climatological conditions, two distinct modes of persistency were found; first one lasting a day or so
287 and dominated by winds from south-easterly direction and the other mode lasting 3 to 5 days
288 dominated by south-westerly and north-westerly winds. This information on the degree of
289 persistency in conjunction with circulation patterns could be useful to identify extreme transport
290 events. Further analysis of circulation patterns in combination with spatial distribution of humidity
291 and its vertical structure suggest that these events occur as a result of long-range transport from
292 southern latitudes, most likely from the northern parts of Germany and France, the Netherlands and
293 Belgium. The analysis presented here provides information that can be used in the process oriented
294 evaluation of chemistry transport models over Scandinavia.

295

296

297 **Acknowledgements**

298

299 We gratefully acknowledge OMI and AIRS Science Team and NASA GES DISC for providing data.
300 The wind data from ERA-Interim reanalysis have been obtained from the ECMWF Data Server.
301 MT acknowledges funding support from the Swedish Clean Air and climate research program of
302 IVL (Swedish Environmental Research Institute). Both MT and AD acknowledge Swedish National
303 Space Board (grants 84/11:1, 84/11:2, Dnr: 94/16).

304

305 **References**

306

307 Beirle, S., Boersma, K. F., Platt, U., Lawrence, M. G., and Wagner, T.: Megacity Emissions and
308 Lifetimes of Nitrogen Oxides Probed from Space, *Science*, 333, 1737–1739,
309 doi:10.1126/science.1207824, 2011.

310

311 Bellander T, Wichmann J, and Lind T., Individual Exposure to NO₂ in Relation to Spatial and
312 Temporal Exposure Indices in Stockholm, Sweden: The INDEX Study. *PLoS ONE* 7(6): e39536.
313 doi:10.1371/journal.pone.0039536, 2009.

314

315 Boersma, K. F., E. J. Bucsela, E. J. Brinkema, J. F. Gleason, NO₂, OMI-EOS Algorithm Theoretical
316 Basis Document: Trace Gas Algorithms: NO₂, 4, 12-35, 2001.
317 http://eosps0.gsfc.nasa.gov/eos_homepage/for_scientists/atbd/docs/OMI/ATBD-OMI-04.pdf
318

319 Boersma, K. F., Jacob, D. J., Bucsela, E. J., Perring, A. E., Dirksen, R., van der A, R. J., Yantosca,
320 R. M., Park, R. J., Wenig, M. O., and Bertram, T. H.: Validation of OMI tropospheric NO₂
321 observations during INTEX-B and application to constrain NO_x emissions over the eastern United
322 States and Mexico, *Atmos. Environ.*, 42, 4480–4497, doi:10.1016/j.atmosenv.2008.02.004, 2008.
323

324 Boersma, K. F., Eskes, H. J., Dirksen, R. J., van der A, R. J., Veefkind, J. P., Stammes, P., Huijnen,
325 V., Kleipool, Q. L., Sneep, M., Claas, J., Leitão, J., Richter, A., Zhou, Y., and Brunner, D.: An
326 improved tropospheric NO₂ column retrieval algorithm for the Ozone Monitoring Instrument,
327 *Atmos. Meas. Tech.*, 4, 1905–1928, doi: 10.5194/amt-4-1905-2011, 2011.
328

329 Bucsela, E. J., Celarier, E. A., Wenig, M. O., Gleason, J. F., Veefkind, J. P., Boersma, K. F., and
330 Brinkema, E. J.: Algorithm for NO₂ vertical column retrieval from the ozone monitoring
331 instrument, *IEEE T. Geosci. Remote*, 44, 1245–1258, doi:10.1109/TGRS.2005.863715, 2006.
332

333 Bucsela, E. J., Perring, A. E., Cohen, R. C., Boersma, K. F., Celarier, E. A., Gleason, J. F., Wenig,
334 M. O., Bertram, T. H., Wooldridge, P. J., Dirksen, R., and Veefkind, J. P.: Comparison of
335 tropospheric NO₂ from in situ aircraft measurements with near-real-time and standard product data
336 from OMI, *J. Geophys. Res.*, 113, D16S31, doi:10.1029/2007JD008838, 2008.
337

338 Bucsela, E. J., Krotkov, N. A., Celarier, E. A., Lamsal, L. N., Swartz, W. H., Bhartia, P. K.,
339 Boersma, K. F., Veefkind, J. P., Gleason, J. F., and Pickering, K. E.: A new stratospheric and
340 tropospheric NO₂ retrieval algorithm for nadir-viewing satellite instruments: applications to OMI,
341 *Atmos. Meas. Tech.*, 6, 2607-2626, doi:10.5194/amt-6-2607-2013, 2013.
342

343 Chahine, M. T and co-authors, AIRS: Improving Weather Forecasting and Providing New Data on
344 Greenhouse Gases, *Bull. Am. Meteorol. Soc.*, 87, 911–926, 2006.
345

346 Dee, D. P., Uppala, S. M., Simmons, A. J., Berrisford, P., Poli, P., Kobayashi, S., Andrae, U.,
347 Balmaseda, M. A., Balsamo, G., Bauer, P., Bechtold, P., Beljaars, A. C. M., van de Berg, L., Bidlot,
348 J., Bormann, N., Delsol, C., Dragani, R., Fuentes, M., Geer, A. J., Haimberger, L., Healy, S. B.,
349 Hersbach, H., Hólm, E. V., Isaksen, L., Kållberg, P., Köhler, M., Matricardi, M., McNally, A. P.,

350 Monge-Sanz, B. M., Morcrette, J.-J., Park, B.-K., Peubey, C., de Rosnay, P., Tavalato, C., Thépaut,
351 J.-N. and Vitart, F.: The ERA-Interim reanalysis: configuration and performance of the data
352 assimilation system. *Q.J.R. Meteorol. Soc.*, 137: 553–597, doi:10.1002/qj.828, 2011.
353

354 Devasthale, A. and M. A. Thomas, An investigation of statistical link between inversion strength
355 and carbon monoxide over Scandinavia in winter using AIRS data, *Atmospheric Environment*, Vol.
356 56, 109-114 s, DOI: 10.1016/j.atmosenv.2012.03.042, 2012.
357

358 Devasthale et al. A decade of space borne observations of the Arctic atmosphere: novel insights
359 from NASA's Atmospheric Infrared Sounder (AIRS) instrument. *Bull. Amer. Meteor. Soc.*
360 doi:10.1175/BAMS-D-14-00202.1, in press, 2016.
361

362 Donnelly, A. A., Broderick, B. M. and Misstear, B. D.: The effect of long-range air mass transport
363 pathways on PM10 and NO2 concentrations at urban and rural background sites in Ireland:
364 Quantification using clustering techniques, *J Environ Sci Health A Tox Hazard Subst Environ Eng.*,
365 doi: 10.1080/10934529.2015.1011955, 2015.
366

367 Eckhardt, S., A. Stohl, S. Beierle, N. Spichtinger, P. James, C. Forster, C. Junker, T. Wagner, U.
368 Platt, and S. G. Jennings, 2003: The North Atlantic Oscillation controls air pollution transport to the
369 Arctic, *Atmos. Chem. Phys.*, 3, 1769-1778, 2003.
370

371 Ehhalt, D. H., Rohrer, F., and Wahner, A.: Sources and Distribution of NO_x in the Upper
372 Troposphere at Northern Mid-Latitudes, *J. Geophys. Res.*, 97, 3725–3738,
373 <http://www.agu.org/journals/jd/v097/iD04/91JD03081/>, 1992.
374

375 Geddes JA, et al. Long-term trends worldwide in ambient NO₂ concentrations inferred from satellite
376 observations. *Environ Health Perspect* 1243281–289.2892016, doi:10.1289/ehp.1409567, 2016.
377

378 Gustafsson, M., H. Orru, B. Forsberg, S. Åström, H. Tekie, K. Sjöberg, Quantification of population
379 exposure to NO₂, PM_{2.5} and PM₁₀ in Sweden 2010, Swedish Environmental Research Institute
380 (IVL), IVL Report B2197, pp. 74, December 2014.
381

382 Klingberg, J., M. P. Björkman, G. P. Karlsson, and H. Pleijel, Observations of Ground-level Ozone
383 and NO₂ in Northernmost Sweden, Including the Scandian Mountain Range, *AMBIO*, 38(8):448-

384 451. doi: <http://dx.doi.org/10.1579/0044-7447-38.8.448>, 2009.

385

386 Lamarque, J.-F. and Dentener, F. and McConnell, J. and Ro, C.-U. and Shaw, M. and Vet, R. and Bergmann,
387 D. and Cameron-Smith, P. and Dalsoren, S. and Doherty, R. and Faluvegi, G. and Ghan, S. J. and Josse, B.
388 and Lee, Y. H. and MacKenzie, I. A. and Plummer, D. and Shindell, D. T. and Skeie, R. B. and Stevenson, D.
389 S. and Strode, S. and Zeng, G. and Curran, M. and Dahl-Jensen, D. and Das, S. and Fritzsche, D. and Nolan,
390 M., Multi-model mean nitrogen and sulfur deposition from the Atmospheric Chemistry and Climate Model
391 Intercomparison Project (ACCMIP): evaluation of historical and projected future changes, *Atmos. Chem.*
392 *Phys.*, 13, 7997-8018, 2013.

393

394 Lamsal LN, Martin RV, van Donkelaar A, Celarier EA, Bucsela EJ, Boersma KF, et al. Indirect
395 validation of tropospheric nitrogen dioxide retrieved from the OMI satellite instrument: insight into
396 the seasonal variation of nitrogen oxides at northern midlatitudes. *J Geophys Res* 115D05302;
397 doi:10.1029/2009JD013351 , 2010.

398

399 Lamsal LN, Martin RV, van Donkelaar A, Steinbacher M, Celarier EA, Bucsela E, et al. Ground-
400 level nitrogen dioxide concentrations inferred from the satellite-borne Ozone Monitoring
401 Instrument. *J Geophys Res* 113D16308; .10.1029/2007JD009235, 2008.

402

403 Lamsal, L. N., Krotkov, N. A., Celarier, E. A., Swartz, W. H., Pickering, K. E., Bucsela, E. J.,
404 Gleason, J. F., Martin, R. V., Philip, S., Irie, H., Cede, A., Herman, J., Weinheimer, A., Szykman, J.
405 J., and Knepp, T. N.: Evaluation of OMI operational standard NO₂ column retrievals using in situ
406 and surface-based NO₂ observations, *Atmos. Chem. Phys.*, 14, 11587-11609, doi:10.5194/acp-14-
407 11587-2014, 2014.

408

409 Nilsson Sommar, J., A. Ek, R. Middelvel, A. Bjerg, S-E. Dahlén, C. Janson, B. Forsberg, Quality
410 of life in relation to the traffic pollution indicators NO₂ and NO_x: results from the Swedish
411 GA2LEN survey, *BMJ Open Resp Res* 2014;1:1 e000039 doi:10.1136/bmjresp-2014-000039.

412

413 Oudin, A., L. Bråbäck, D. Oudin Åström, M. Strömgren, and B. Forsberg, Association between
414 neighbourhood air pollution concentrations and dispensed medication for psychiatric disorders in a
415 large longitudinal cohort of Swedish children and adolescents, *BMJ Open* 2016;6:6 e010004
416 doi:10.1136/bmjopen-2015-010004, 2016.

417

418 Richter A, Burrows JP, Nüss H, Granier C, Niemeier U. Increase in tropospheric nitrogen dioxide
419 over China observed from space. *Nature* 437129–132.132; doi:10.1038/nature04092, 2005.

420

421 Schneider, P., Lahoz, W. A., and van der A, R.: Recent satellite-based trends of tropospheric
422 nitrogen dioxide over large urban agglomerations worldwide, *Atmos. Chem. Phys.*, 15, 1205-1220,
423 doi:10.5194/acp-15-1205-2015, 2015.

424

425 Sjöberg K., M. Haeger-Eugensson, M. Lijeberg, H. Blomgren, and B. Forsberg, Quantification of
426 population exposure to nitrogen dioxide in Sweden, Swedish Environmental Research Institute
427 (IVL), IVL Report B1579, pp. 31, September 2004.

428

429 Stohl, A., Huntrieser, H., Richter, A., Beirle, S., Cooper, O. R., Eckhardt, S., Forster, C., James, P.,
430 Spichtinger, N., and Wenig, M.: Rapid intercontinental air pollution transport associated with a
431 meteorological bomb, *Atmos. Chem. Phys.*, 3, 969–985, 2003, [http://www.atmos-chem-](http://www.atmos-chem-phys.net/3/969/2003/)
432 [phys.net/3/969/2003/](http://www.atmos-chem-phys.net/3/969/2003/).

433

434 Schaub, D., Weiss, A. K., Kaiser, J. W., Petritoli, A., Richter, A., Buchmann, B., and Burrows, J. P.:
435 A transboundary transport episode of nitrogen dioxide as observed from GOME and its impact in
436 the Alpine region, *Atmos. Chem. Phys.*, 5, 23–37, doi:10.5194/acp-5-23-2005, 2005.

437

438 Susskind, J., J. M. Blaisdell and L. Iredell, Improved methodology for surface and atmospheric
439 soundings, error estimates and quality control procedures: the atmospheric infrared sounder science
440 team version-6 retrieval algorithm, *J. Appl. Remote Sens.*, 8(1), 084994,
441 doi:10.1117/1.JRS.8.084994, 2014.

442

443 Taj T, Stroh E, Åström DO, Jakobsson K, Oudin A., Short-Term Fluctuations in Air Pollution and
444 Asthma in Scania, Sweden. Is the Association Modified by Long-Term Concentrations? *PLoS ONE*
445 11(11): e0166614. doi:10.1371/journal.pone.0166614, 2016.

446

447 Thomas, M. A. and Devasthale, A.: Sensitivity of free tropospheric carbon monoxide to atmospheric
448 weather states and their persistency: an observational assessment over the Nordic countries, *Atmos.*
449 *Chem. Phys.*, 14, 11545-11555, doi:10.5194/acp-14-11545-2014, 2014.

450

451 van der A, R. J., H. J. Eskes, K. F. Boersma, T. P. C. van Noije, M. Van Roozendaal, I. De Smedt, D.
452 H. M. U. Peters, and E. W. Meijer, Trends, seasonal variability and dominant NO_x source derived

453 from a ten year record of NO₂ measured from space, *J. Geophys. Res.*, 113, D04302,
454 doi:10.1029/2007JD009021, 2008.

455

456 Vasilkov, A. P., Joiner, J., Oreopoulos, L., Gleason, J. F., Veefkind, P., Bucsela, E., Celarier, E. A.,
457 Spurr, R. J. D., and Platnick, S.: Impact of tropospheric nitrogen dioxide on the regional radiation
458 budget, *Atmos. Chem. Phys.*, 9, 6389-6400, doi:10.5194/acp-9-6389-2009, 2009.

459

460 Wenig, M., Spichtinger, N., Stohl, A., Held, G., Beirle, S., Wagner, T., Jähne, B., and Platt, U.:
461 Intercontinental transport of nitrogen oxide pollution plumes, *Atmos. Chem. Phys.*, 3, 387–393,
462 doi:10.5194/acp-3-387-2003, 2003.

463

464 Zhang, Q., et al., NO_x emission trends for China, 1995–2004: The view from the ground and the
465 view from space, *J. Geophys. Res.*, 112, D22306, doi:10.1029/2007JD008684, 2007.

466

467 Zien, A. W., Richter, A., Hilboll, A., Blechschmidt, A.-M., and Burrows, J. P.: Systematic analysis
468 of tropospheric NO₂ long-range transport events detected in GOME-2 satellite data, *Atmos. Chem.*
469 *Phys.*, 14, 7367–7396, doi: 10.5194/acp-14-7367-2014, 2014.

470

471

472

473

474

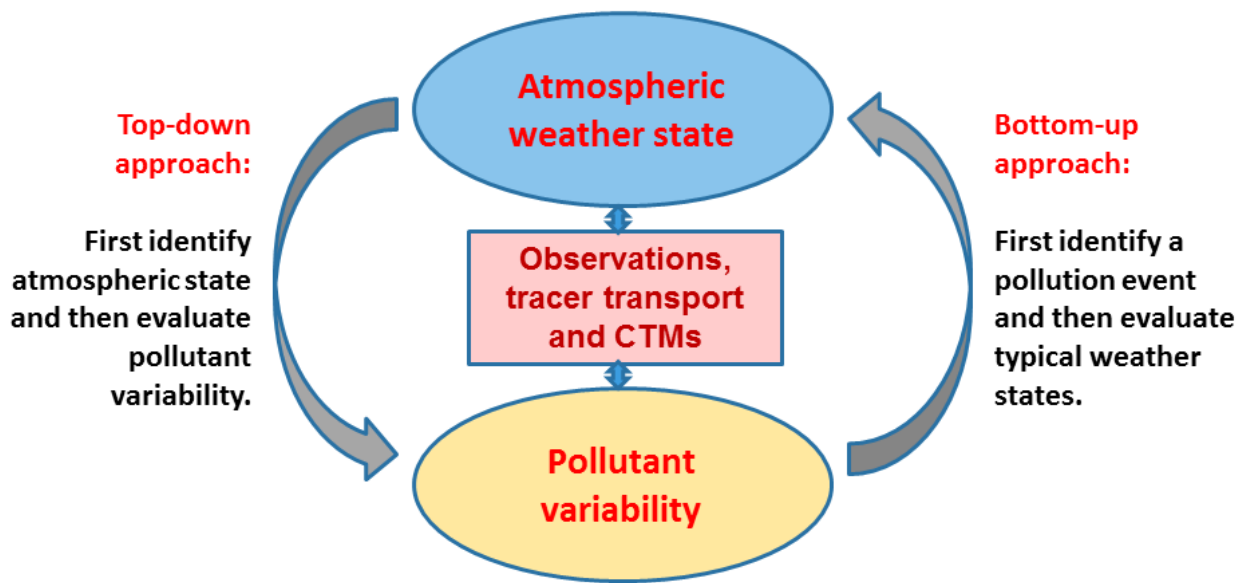
475

476

477

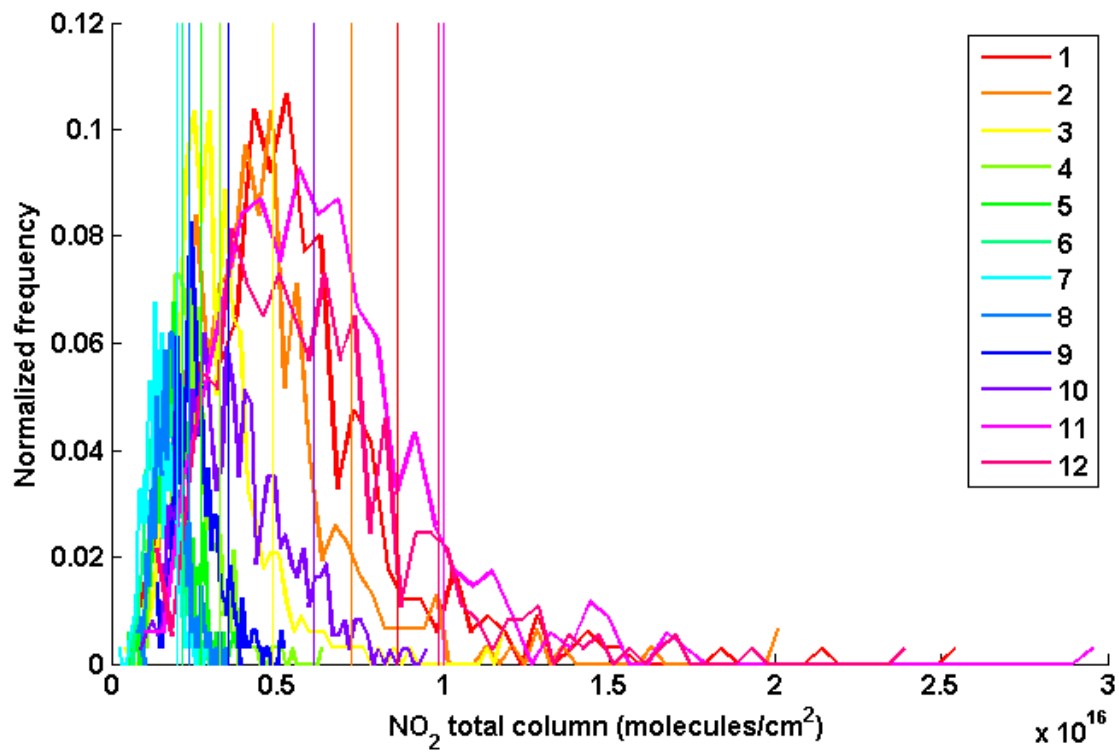
478

479



480
 481 Fig. 1: Schematic showing two different approaches to study statistical co-variability of
 482 atmospheric weather states and pollutant concentrations.

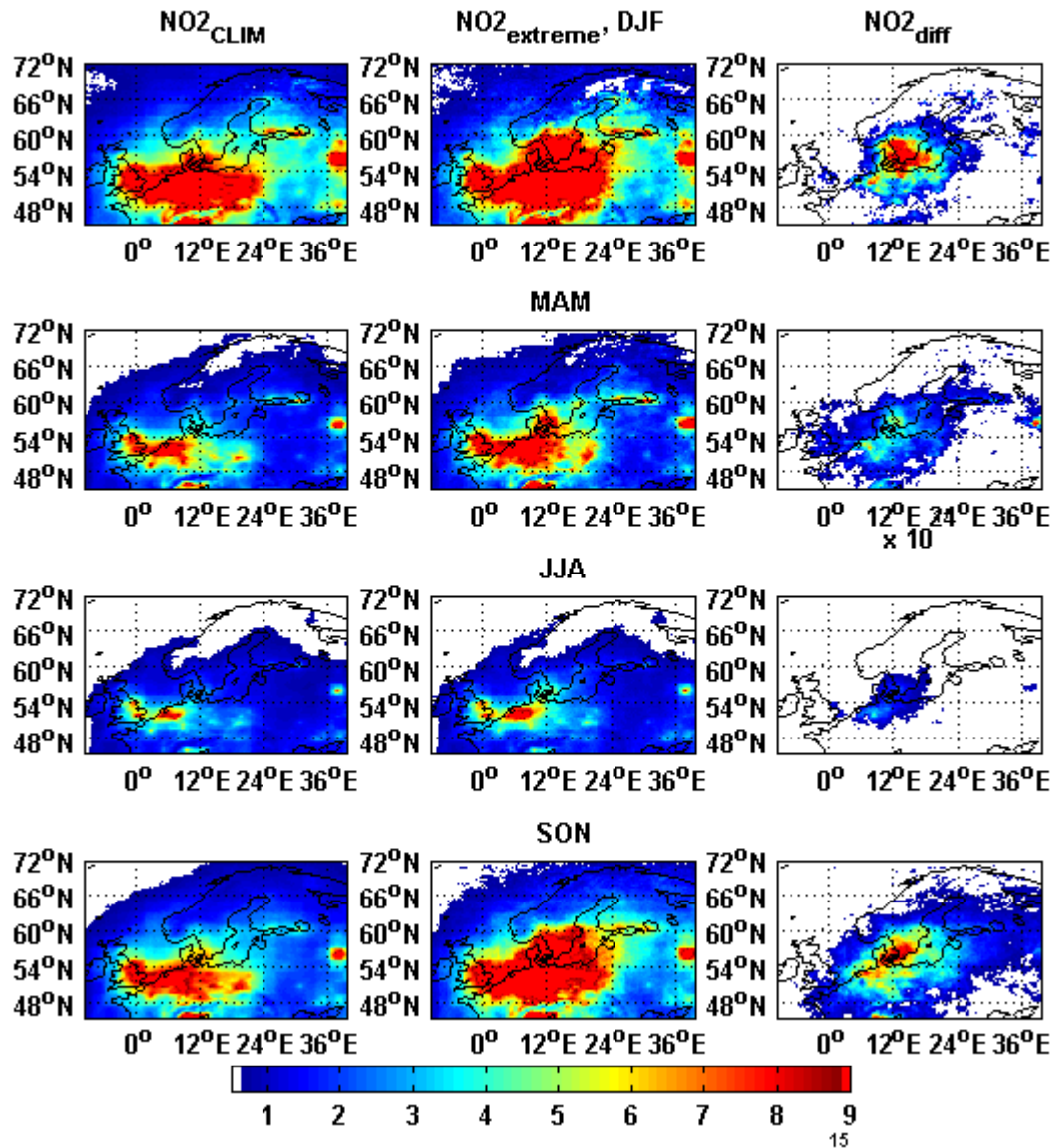
483
 484
 485
 486
 487
 488
 489
 490
 491
 492
 493
 494
 495
 496
 497



498

499

500 Fig. 2: Monthly histograms of tropospheric total column NO₂ over the centre of the study area
 501 (55N-60N, 11E-20E) and corresponding 90%ile thresholds (shown by vertical lines). The legend
 502 shows the month number from starting January to December.



503

504

505 Fig, 3: Seasonal, climatological average tropospheric NO₂ total column (first column) based on
 506 nearly 11-yr OMI data (2004-2015), NO₂ distribution during extreme events (second column) and
 507 the difference between the two (third column). The units are in molecules/cm².

508

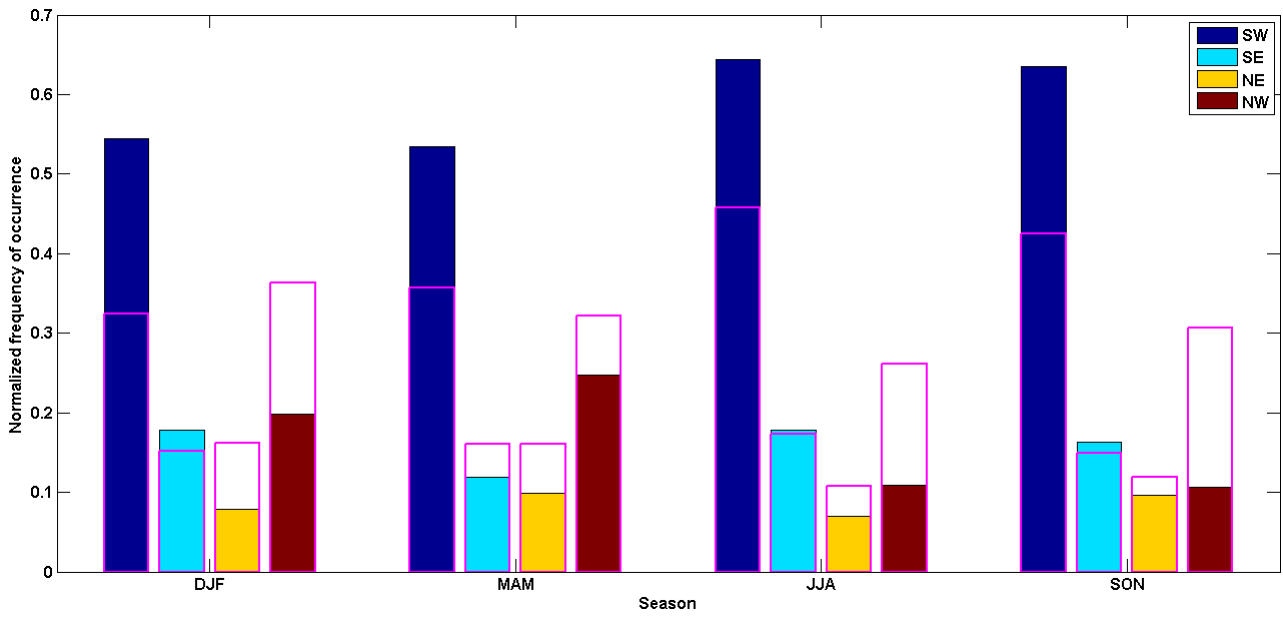
509

510

511

512

513



514

515

516

517 Fig. 4: Seasonal normalized frequency of occurrence of a particular wind direction at 850 hPa when
 518 NO₂ extreme pollution events were observed. The hollow magenta bars show normalized frequency
 519 under climatological conditions.

520

521

522

523

524

525

526

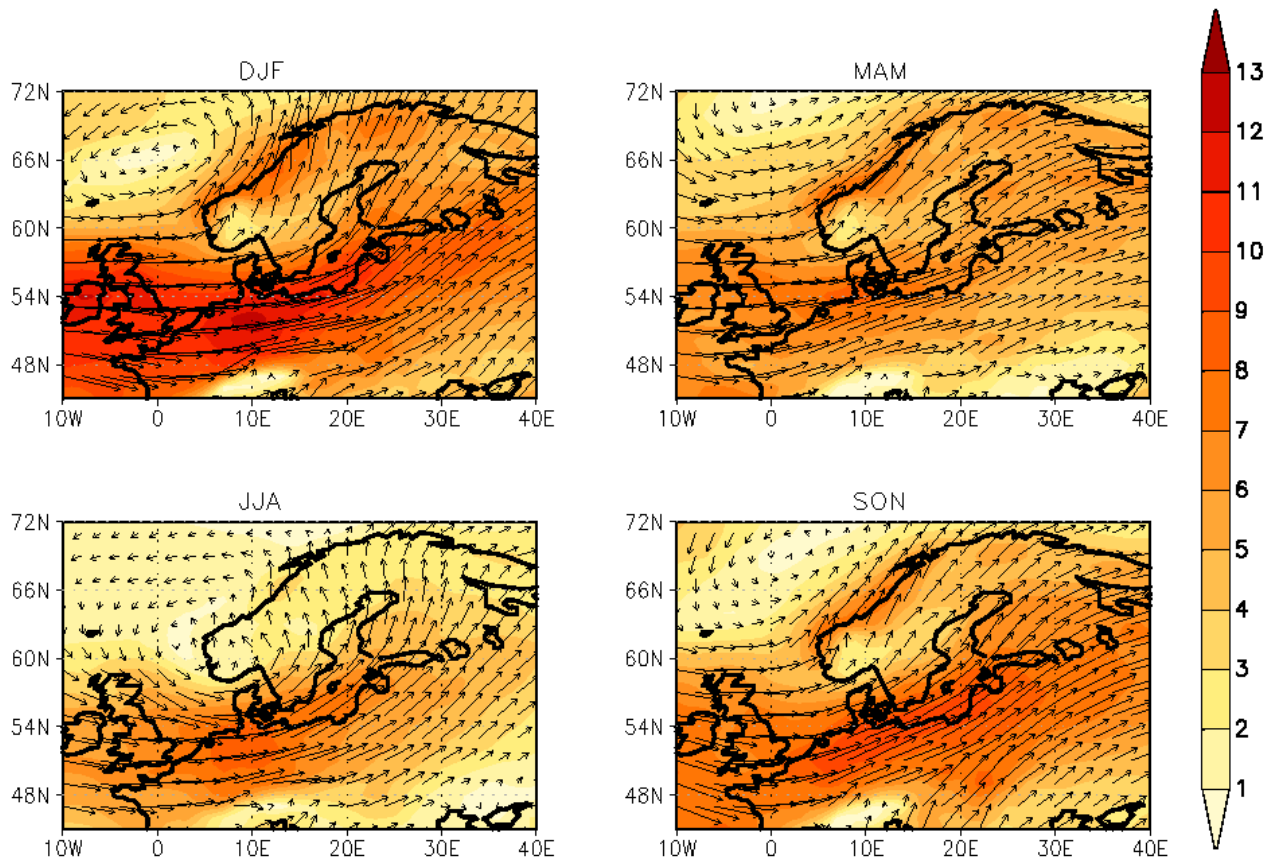
527

528

529

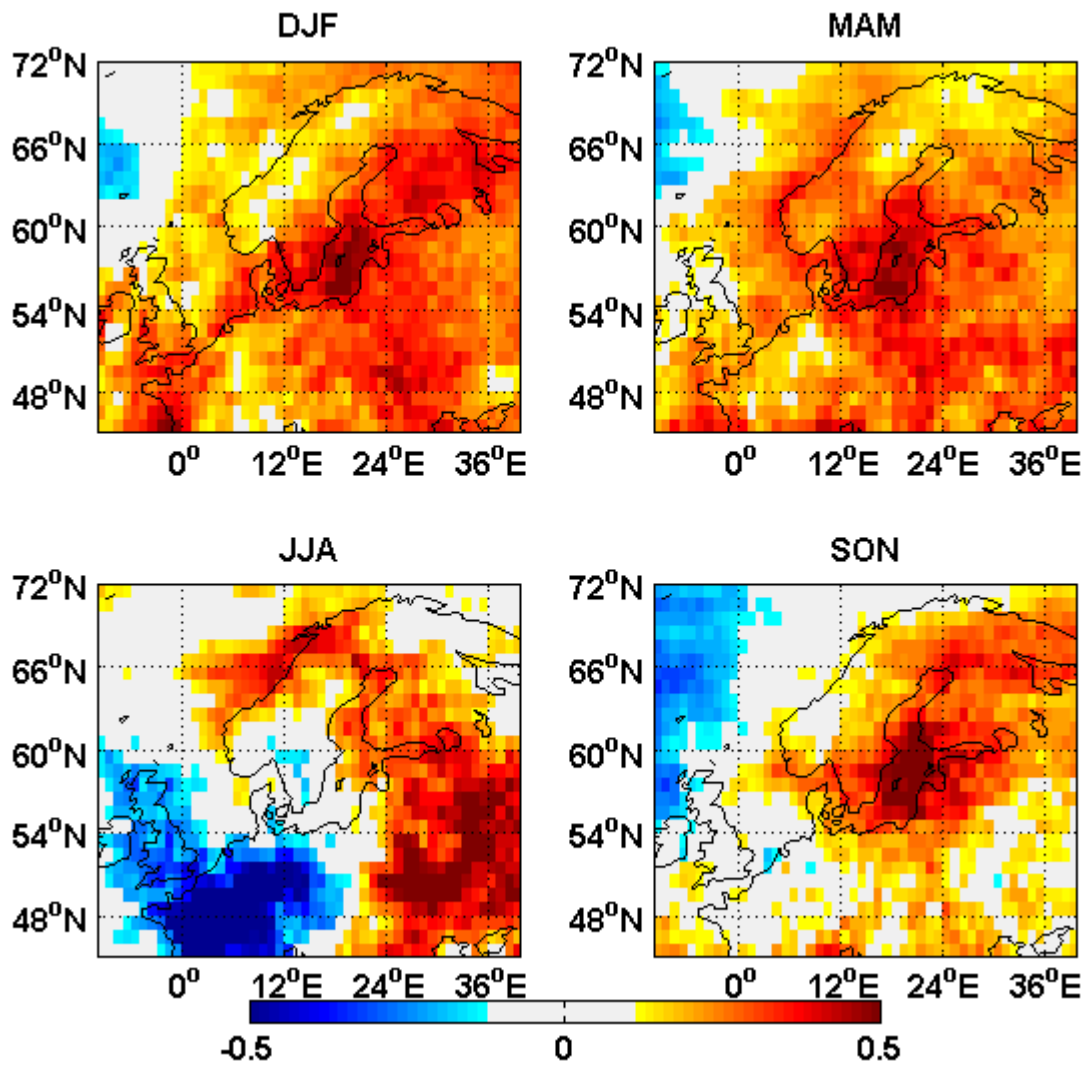
530

531



532
 533
 534
 535
 536
 537
 538

Fig. 5: Seasonal average wind strengths and direction at 850 hPa showing dominant circulation pattern observed when NO₂ extreme pollution events occur.



539

540

541 Fig. 6: The seasonal spatial patterns of specific humidity anomalies (g/kg) during extreme NO₂
 542 pollution events.

543

544

545

546

547

548

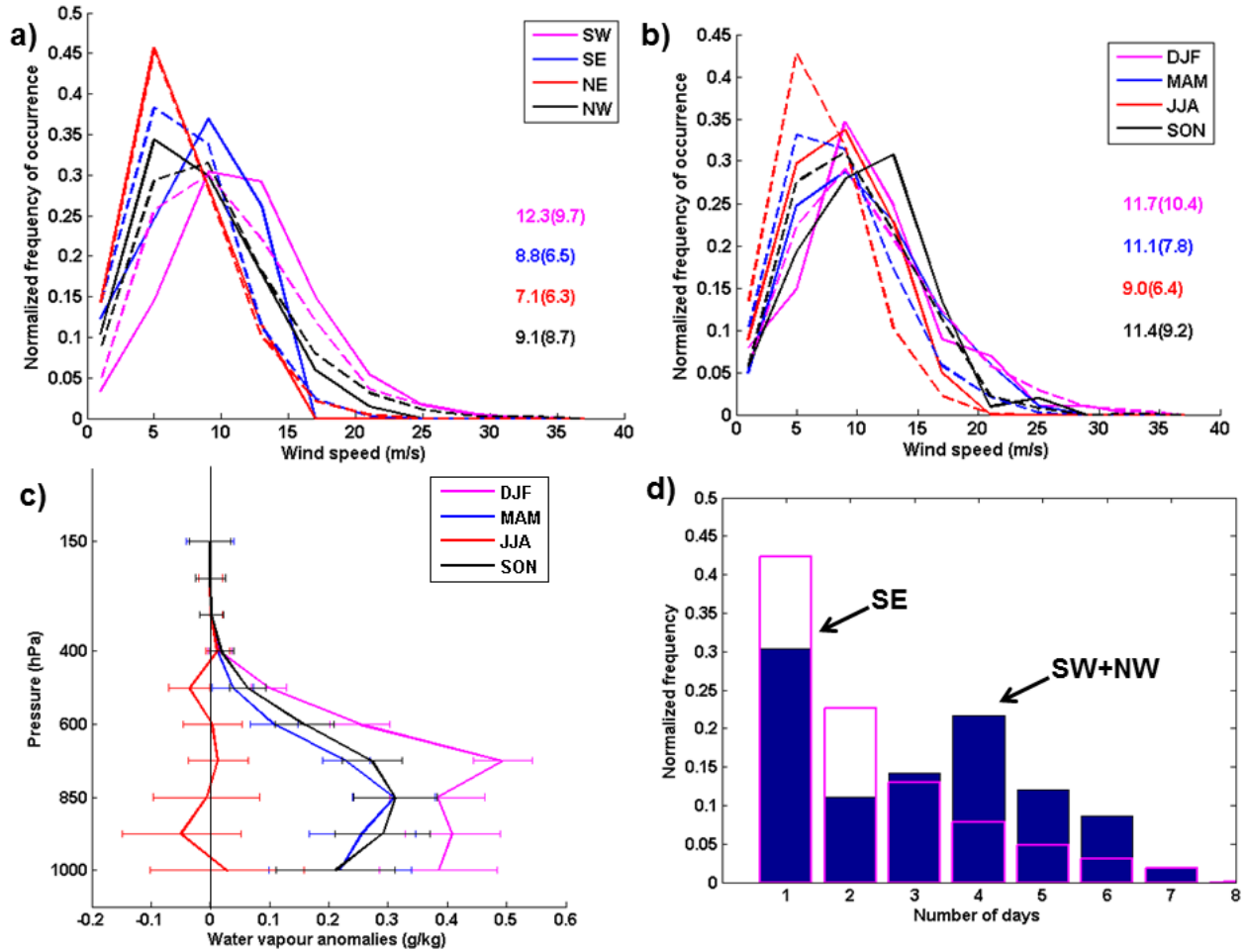
549

550

551

552

553



555

556

557 Fig. 7: a) Histograms of wind speeds (m/s) at 850 hPa over the center of the study area (55N-60N,

558 11E-20E) during extreme events (solid lines) and climatological conditions (dotted lines, 2004-

559 2015) when data are partitioned for different wind directions. The numbers show average wind

560 speeds (m/s) during extreme events and in brackets under climatological conditions. b) Same as in

561 (a), but when wind data are partitioned for different seasons. c) Vertical anomalies of specific

562 humidity (g/kg) during extreme events with horizontal bars showing standard deviations. d)

563 Persistency of wind directions as a function of number of continuous days. The magenta bars show

564 persistency under climatological conditions.

565

566

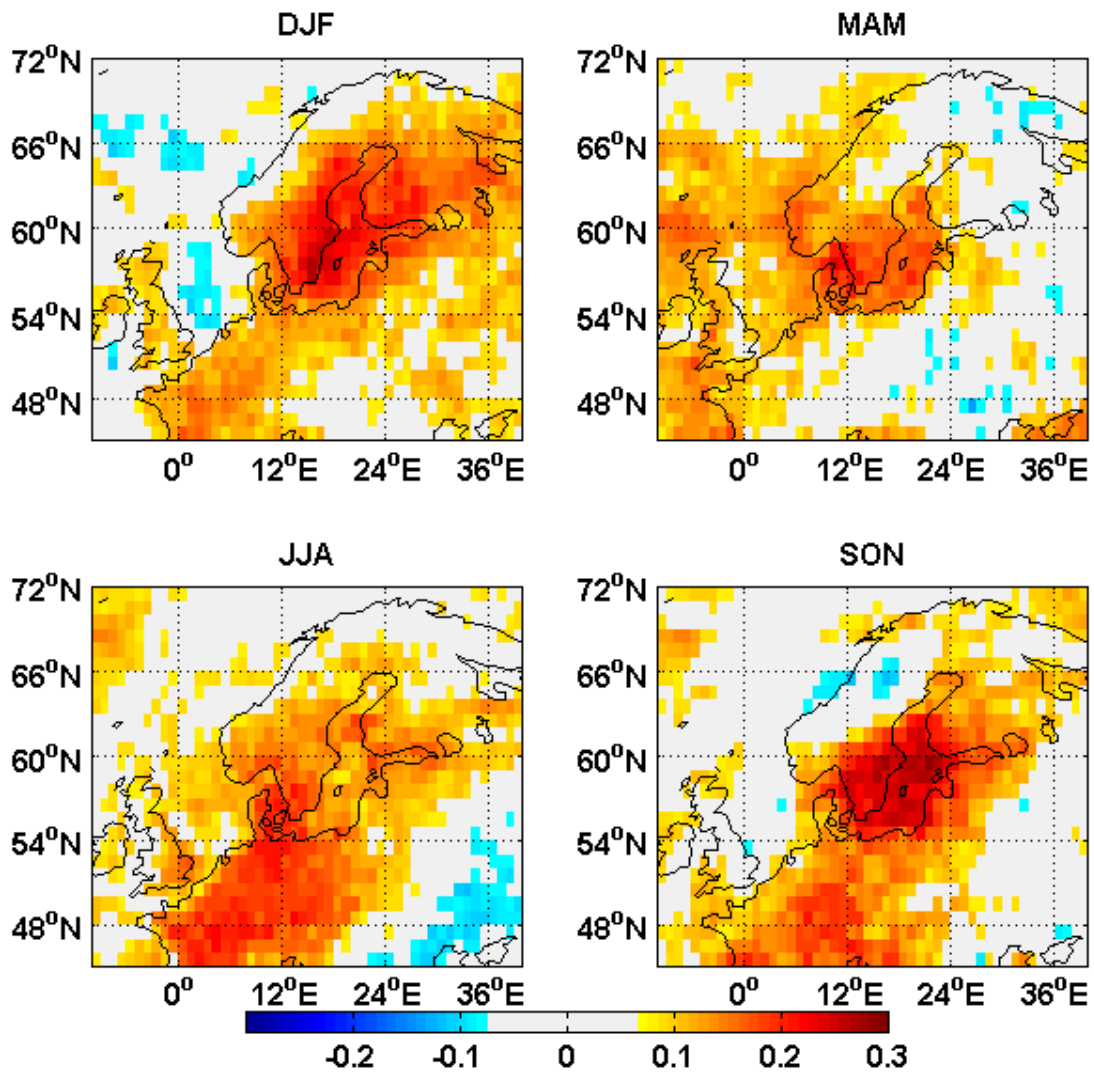
567

568

569

570

571



572

573

574 Fig. 8: Total cloud fraction anomalies observed during extreme events based on AIRS data.

575

576

577

578

579

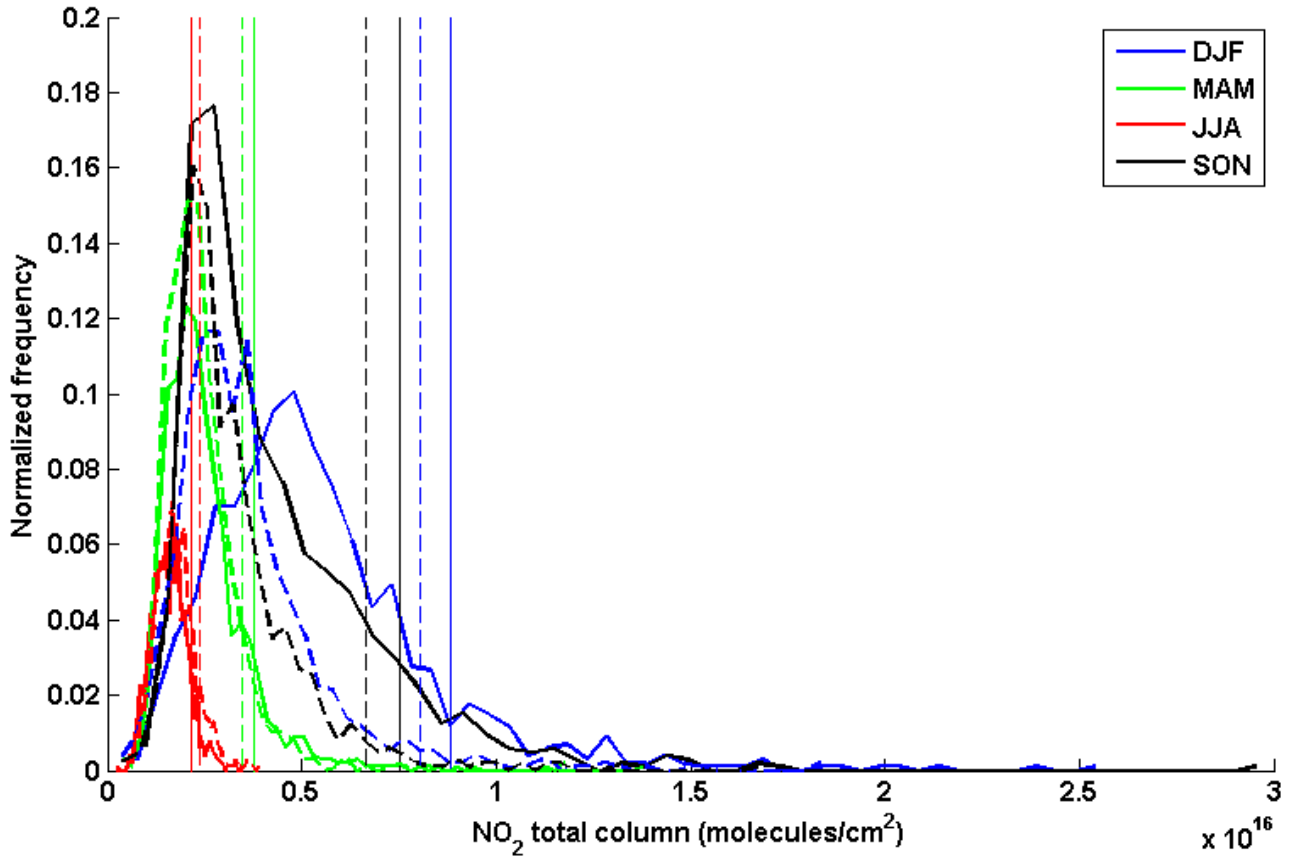
580

581

582

583

584
585
586
587

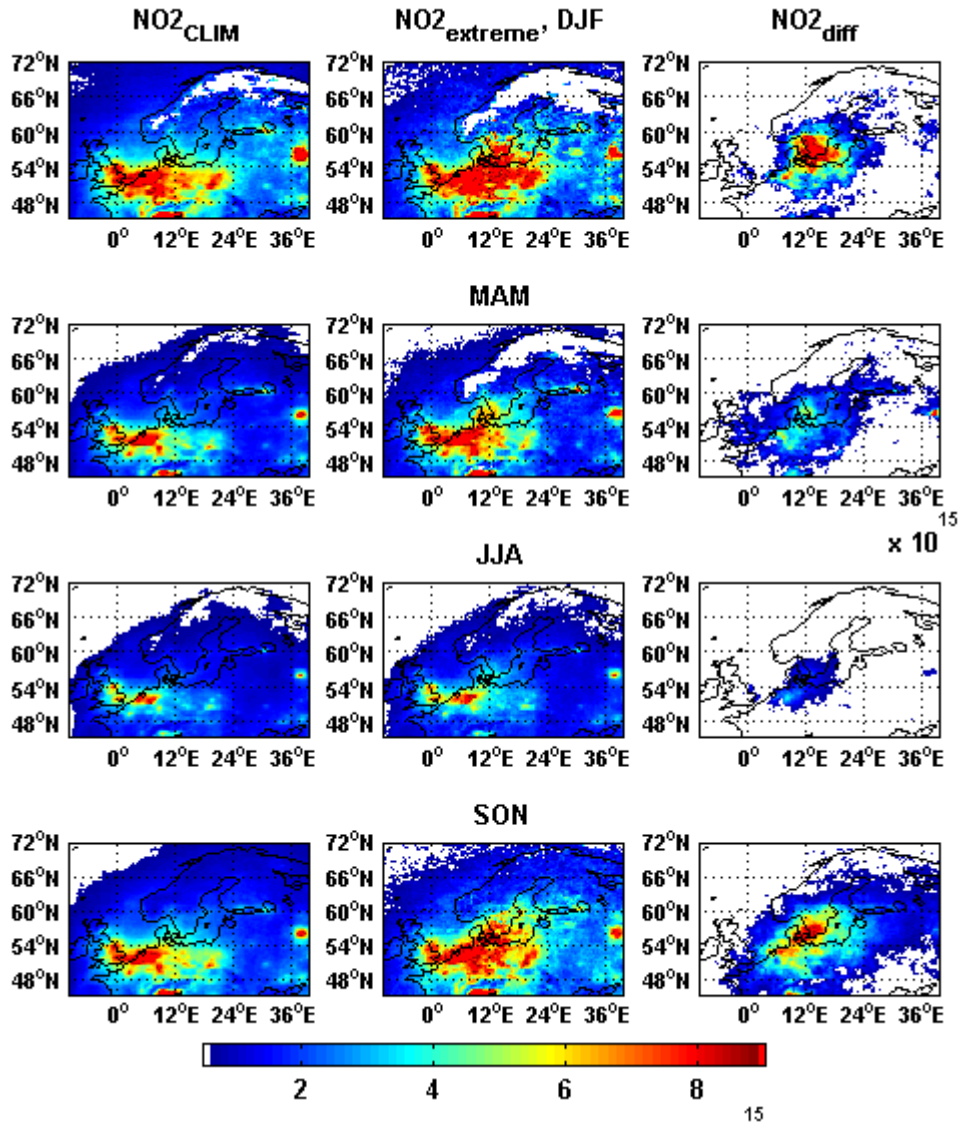


588
589

590 Fig. 9: Seasonal histograms of total column tropospheric NO₂ over the centre of the study area
591 (55N-60N, 11E-20E) and corresponding 90%ile thresholds (shown by vertical lines). The solid lines
592 show histograms based on retrievals under partially cloudy conditions, while the dotted lines show
593 histograms based only on cloud cleared retrievals.

594
595
596
597
598
599

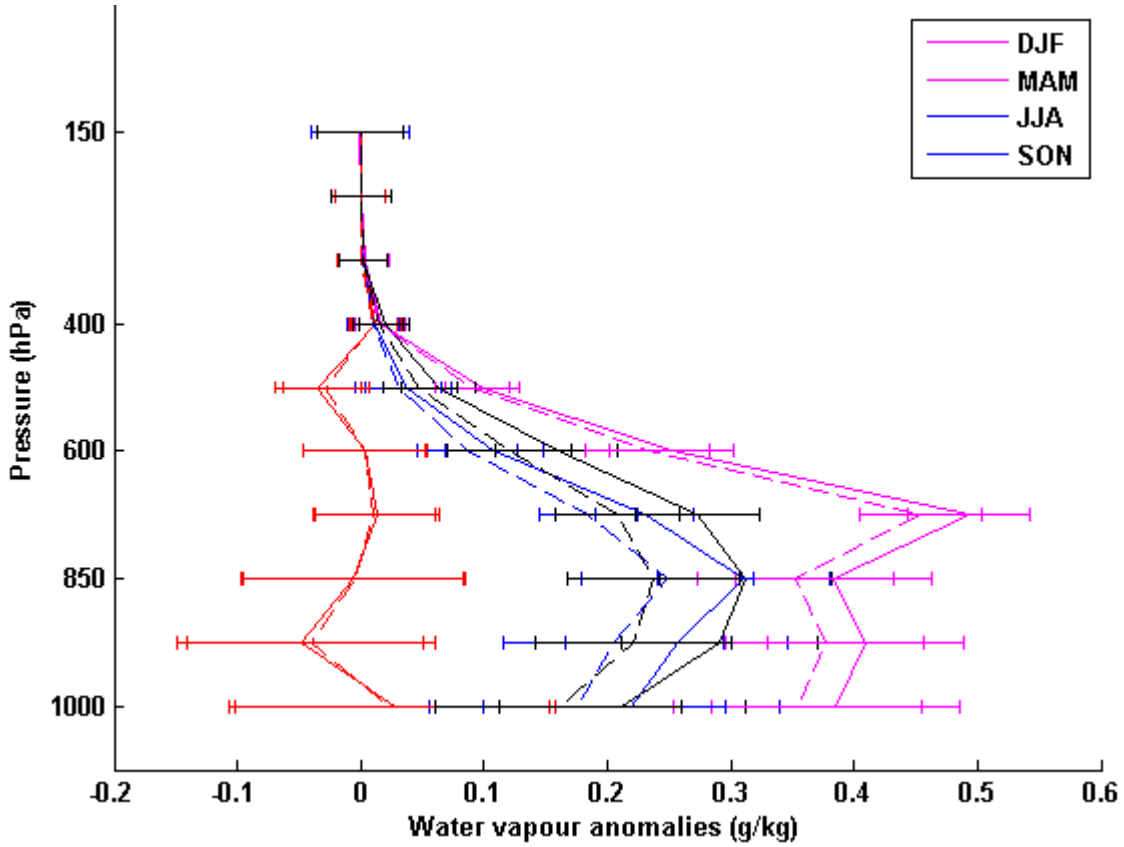
600
601
602
603



604
605
606
607
608
609
610
611

Fig. 10: Seasonal, climatological average tropospheric NO₂ total column (first column) based only on cloud screened OMI data (2004-2015), NO₂ distribution during extreme events (second column, also based on cloud screened data) and the difference between the two (third column). The units are in molecules/cm².

612
613
614
615



616
617
618
619
620
621

Fig. 11: Vertical anomalies of specific humidity (g/kg) during extreme events with horizontal bars showing standard deviations. The solid lines show anomalies under partially cloudy retrievals and dotted lines based on cloud screened retrievals.